

The “pogo stick” complex [FeCp*{N(SiMe₃)₂}] : spin state properties, adduct formation with Lewis bases, and reactivity towards weakly Brønsted acidic protonated NHCs

Julian Zinke,^a Clemens Bruhn,^a Serhiy Demeshko^b and Ulrich Siemeling^{*a}

^a *Institute of Chemistry, University of Kassel, Heinrich-Plett-Straße 40, 34132 Kassel, Germany. E-mail: siemeling@uni-kassel.de*

^b *Institut für Anorganische Chemie, Georg-August-Universität Göttingen, Tammannstraße 4, 37077 Göttingen, Germany*

A	X-Ray crystallography	S2
B	Plots of NMR spectra	S4
C	Mößbauer spectroscopy	S8
D	Magnetic measurements	S8
E	References	S11

A X-ray crystallography

Table S1 Crystal data and structure refinement details

	1	1·0.5 benzene	2	3·1.5 benzene	4	5·2 toluene	6
Empirical formula	C ₃₇ H ₅₁ ClFeN ₂	C ₄₀ H ₅₄ ClFeN ₂	C ₁₉ H ₂₅ FeIN ₂	C ₄₄ H ₅₆ Fe ₂ I ₂ N ₄	C ₄₁ H ₄₉ ClFe ₂ N ₂	C ₅₅ H ₆₆ Cl ₂ Fe ₂ N ₂	C ₂₃ H ₄₃ FeN ₃ Si ₂
Formula weight	615.09	654.15	464.16	1006.42	716.97	937.69	473.63
Crystal system	orthorhombic	monoclinic	triclinic	monoclinic	orthorhombic	triclinic	monoclinic
Space group	<i>Aea</i> 2	<i>P</i> 2 ₁ / <i>n</i>	<i>P</i> -1	<i>P</i> 2 ₁ / <i>c</i>	<i>Pnma</i>	<i>P</i> -1	<i>Cc</i>
<i>a</i> /Å	23.6175(8)	11.6577(3)	14.1651(10)	12.595(2)	16.928(2)	12.5906(7)	18.9537(4)
<i>b</i> /Å	17.8626(5)	20.9198(4)	17.6905(12)	27.760(2)	20.7331(15)	14.1602(7)	19.2088(4)
<i>c</i> /Å	16.2168(4)	15.6499(4)	22.2919(16)	14.5083(14)	10.0628(11)	15.1245(8)	29.7352(6)
α /°	90	90	67.201(5)	90	90	70.092(4)	90
β /°	90	102.915(2)	72.354(6)	115.625(11)	90	89.668(4)	98.754(2)
γ /°	90	90	70.236(5)	90	90	73.820(4)	90
Volume/Å ³	6841.4(3)	3720.10(16)	4750.0(6)	4573.7(10)	3531.7(7)	2423.0(2)	10699.8(4)
<i>Z</i>	8	4	10	4	4	2	16
ρ_{calc} /gcm ⁻³	1.194	1.168	1.623	1.462	1.348	1.285	1.176
μ /mm ⁻¹	4.437	4.109	2.420	2.017	7.510	6.093	0.667
<i>F</i> (000)	2640.0	1404.0	2320.0	2024.0	1512.0	992.0	4096.0
Crystal size/mm ³	0.23 × 0.17 × 0.09	0.28 × 0.26 × 0.05	0.19 × 0.13 × 0.08	0.19 × 0.11 × 0.04	0.09 × 0.06 × 0.05	0.16 × 0.08 × 0.03	0.32 × 0.24 × 0.11
Radiation used	CuK α (λ = 1.54186)	CuK α (λ = 1.54186)	MoK α (λ = 0.71073)	MoK α (λ = 0.71073)	CuK α (λ = 1.54186)	CuK α (λ = 1.54186)	MoK α (λ = 0.71073)
2 θ range for data collection/°	7.486 to 141.998	7.172 to 137.952	2.58 to 52.032	3.442 to 51.746	8.53 to 142.636	6.246 to 142.02	2.772 to 51.998
	-21 ≤ <i>h</i> ≤ 28	-14 ≤ <i>h</i> ≤ 13	-17 ≤ <i>h</i> ≤ 16	-15 ≤ <i>h</i> ≤ 15	-20 ≤ <i>h</i> ≤ 20	-14 ≤ <i>h</i> ≤ 15	-23 ≤ <i>h</i> ≤ 23
Index ranges	-21 ≤ <i>k</i> ≤ 21	-17 ≤ <i>k</i> ≤ 25	-21 ≤ <i>k</i> ≤ 21	-29 ≤ <i>k</i> ≤ 34	-11 ≤ <i>k</i> ≤ 24	-15 ≤ <i>k</i> ≤ 17	-23 ≤ <i>k</i> ≤ 23
	-19 ≤ <i>l</i> ≤ 13	-18 ≤ <i>l</i> ≤ 14	-24 ≤ <i>l</i> ≤ 27	-17 ≤ <i>l</i> ≤ 15	-12 ≤ <i>l</i> ≤ 11	-18 ≤ <i>l</i> ≤ 11	-36 ≤ <i>l</i> ≤ 35
Reflections collected	48105	25427	34029	18314	11672	22014	30799
Independent reflections	5149 [<i>R</i> _{int} = 0.0261]	6838 [<i>R</i> _{int} = 0.0380]	17998 [<i>R</i> _{int} = 0.0447]	8713 [<i>R</i> _{int} = 0.0410]	3429 [<i>R</i> _{int} = 0.0718]	8991 [<i>R</i> _{int} = 0.0542]	18847 [<i>R</i> _{int} = 0.0597]
Data/restraints/parameters	5149/1/383	6838/2/410	17998/0/1037	8713/0/483	3429/3/227	8991/0/563	18847/2/1098
Goodness-of-fit on <i>F</i> ²	1.037	1.107	1.173	1.026	1.026	1.059	1.051
Final <i>R</i> indexes	<i>R</i> 1 = 0.0244	<i>R</i> 1 = 0.0459	<i>R</i> 1 = 0.0689	<i>R</i> 1 = 0.0528	<i>R</i> 1 = 0.0692	<i>R</i> 1 = 0.0631	<i>R</i> 1 = 0.0619
[<i>I</i> > 2 σ (<i>I</i>)]	<i>wR</i> 2 = 0.0602	<i>wR</i> 2 = 0.1049	<i>wR</i> 2 = 0.1398	<i>wR</i> 2 = 0.1333	<i>wR</i> 2 = 0.1737	<i>wR</i> 2 = 0.1413	<i>wR</i> 2 = 0.1589
Final <i>R</i> indexes	<i>R</i> 1 = 0.0266	<i>R</i> 1 = 0.0619	<i>R</i> 1 = 0.1111	<i>R</i> 1 = 0.0746	<i>R</i> 1 = 0.0890	<i>R</i> 1 = 0.0987	<i>R</i> 1 = 0.0744
[all data]	<i>wR</i> 2 = 0.0616	<i>wR</i> 2 = 0.1158	<i>wR</i> 2 = 0.1747	<i>wR</i> 2 = 0.1513	<i>wR</i> 2 = 0.1925	<i>wR</i> 2 = 0.1593	<i>wR</i> 2 = 0.1910
Residual electron density/eÅ ⁻³	0.18/-0.26	0.48/-0.33	2.79/-4.68	0.83/-1.31	1.20/-0.49	1.18/-0.38	1.13/-0.87
Flack parameter	-0.012(3)						0.01(2)
CCDC No.	2421670	2421671	2421672	2421673	2421674	2421675	2421676

Table S1 (continued) Crystal data and structure refinement details

	7	8-0.5 benzene	9	10	11	12	13-THF
Empirical formula	C ₂₈ H ₆₁ ClFeN ₂ Si ₂	C ₃₁ H ₆₄ BrFeN ₂ Si ₂	C ₄₇ H ₆₈ BrFe ₂ N ₃ Si ₂	C ₄₁ H ₄₉ BrFe ₂ N ₂	C ₃₅ H ₃₇ ClFe ₂ N ₂	C ₃₅ H ₃₇ BrFe ₂ N ₂	C ₆₄ H ₆₇ F ₆ Fe ₃ N ₄ OP
Formula weight	573.26	656.78	922.83	761.43	632.81	677.27	1220.73
Crystal system	monoclinic	monoclinic	triclinic	orthorhombic	monoclinic	monoclinic	triclinic
Space group	<i>P</i> 2 ₁ / <i>n</i>	<i>C</i> 2/ <i>c</i>	<i>P</i> -1	<i>Pnma</i>	<i>P</i> 2 ₁ / <i>n</i>	<i>P</i> 2 ₁ / <i>n</i>	<i>P</i> 1
<i>a</i> /Å	11.0667(4)	31.820(2)	16.6856(11)	17.0770(7)	10.6053(6)	10.7264(4)	11.2935(9)
<i>b</i> /Å	17.2682(7)	15.1513(7)	17.8813(10)	20.6820(7)	19.0292(8)	18.7784(6)	11.4184(9)
<i>c</i> /Å	19.6530(7)	26.4423(16)	17.8666(11)	10.0448(4)	14.8035(8)	14.9961(5)	12.7670(10)
α /°	90	90	111.389(4)	90	90	90	87.754(6)
β /°	100.046(3)	141.300(3)	90.280(5)	90	92.581(4)	94.026(3)	70.742(6)
γ /°	90	90	107.295(5)	90	90	90	61.971(6)
Volume/Å ³	3698.1(2)	7970.8(9)	4700.5(5)	3547.7(2)	2984.5(3)	3013.13(18)	1358.6(2)
<i>Z</i>	4	8	4	4	4	4	1
$\rho_{\text{calcd}}/\text{gcm}^{-3}$	1.030	1.095	1.304	1.426	1.408	1.493	1.492
μ/mm^{-1}	0.561	1.460	1.552	8.103	1.089	2.316	0.889
<i>F</i> (000)	1256.0	2824.0	1944.0	1584.0	1320.0	1392.0	634.0
Crystal size/mm ³	0.30 × 0.16 × 0.09	0.19 × 0.11 × 0.05	0.27 × 0.20 × 0.12	0.17 × 0.09 × 0.03	0.24 × 0.15 × 0.07	0.2 × 0.16 × 0.13	0.15 × 0.09 × 0.03
Radiation used	MoK α (λ = 0.71073)	MoK α (λ = 0.71073)	MoK α (λ = 0.71073)	CuK α (λ = 1.54186)	MoK α (λ = 0.71073)	MoK α (λ = 0.71073)	MoK α (λ = 0.71073)
2 θ range for data collection/°	3.956 to 51.624	4.466 to 55.998	4.144 to 54	8.55 to 141.908	3.488 to 51.462	3.48 to 51.472	3.412 to 52.002
	-13 ≤ <i>h</i> ≤ 12	-31 ≤ <i>h</i> ≤ 42	-21 ≤ <i>h</i> ≤ 18	-12 ≤ <i>h</i> ≤ 20	-12 ≤ <i>h</i> ≤ 12	-13 ≤ <i>h</i> ≤ 13	-13 ≤ <i>h</i> ≤ 13
Index ranges	-21 ≤ <i>k</i> ≤ 20	-9 ≤ <i>k</i> ≤ 19	-18 ≤ <i>k</i> ≤ 22	-25 ≤ <i>k</i> ≤ 18	-23 ≤ <i>k</i> ≤ 22	-22 ≤ <i>k</i> ≤ 20	-13 ≤ <i>k</i> ≤ 13
	-23 ≤ <i>l</i> ≤ 23	-34 ≤ <i>l</i> ≤ 32	-22 ≤ <i>l</i> ≤ 21	-8 ≤ <i>l</i> ≤ 12	-18 ≤ <i>l</i> ≤ 18	-18 ≤ <i>l</i> ≤ 15	-15 ≤ <i>l</i> ≤ 15
Reflections collected	21020	19715	34993	9189	17094	12245	28334
Independent reflections	7046 [<i>R</i> _{int} = 0.0743]	9536 [<i>R</i> _{int} = 0.0445]	20060 [<i>R</i> _{int} = 0.0585]	3440 [<i>R</i> _{int} = 0.0357]	5633 [<i>R</i> _{int} = 0.0565]	5690 [<i>R</i> _{int} = 0.0231]	9902 [<i>R</i> _{int} = 0.0590]
Data/restraints/parameters	7046/0/323	9536/0/421	20060/174/1103	3440/30/228	5633/0/366	5690/0/366	9902/66/663
Goodness-of-fit on <i>F</i> ²	1.133	1.017	1.006	1.037	1.220	1.058	1.033
Final <i>R</i> indexes	<i>R</i> 1 = 0.0586	<i>R</i> 1 = 0.0542	<i>R</i> 1 = 0.0578	<i>R</i> 1 = 0.0432	<i>R</i> 1 = 0.0656	<i>R</i> 1 = 0.0306	<i>R</i> 1 = 0.0871
[<i>I</i> > 2 σ (<i>I</i>)]	<i>wR</i> 2 = 0.1676	<i>wR</i> 2 = 0.0973	<i>wR</i> 2 = 0.1253	<i>wR</i> 2 = 0.1017	<i>wR</i> 2 = 0.1836	<i>wR</i> 2 = 0.0753	<i>wR</i> 2 = 0.1904
Final <i>R</i> indexes	<i>R</i> 1 = 0.0719	<i>R</i> 1 = 0.1075	<i>R</i> 1 = 0.1088	<i>R</i> 1 = 0.0605	<i>R</i> 1 = 0.0920	<i>R</i> 1 = 0.0380	<i>R</i> 1 = 0.1349
[all data]	<i>wR</i> 2 = 0.1780	<i>wR</i> 2 = 0.1165	<i>wR</i> 2 = 0.1491	<i>wR</i> 2 = 0.1112	<i>wR</i> 2 = 0.2614	<i>wR</i> 2 = 0.0802	<i>wR</i> 2 = 0.2217
Residual electron density/eÅ ⁻³	0.55/−0.71	0.48/−0.37	0.66/−0.66	0.51/−0.66	1.15/−1.16	0.60/−0.24	1.78/−0.85
Flack parameter							0.003(15)
CCDC No.	2421677	2421678	2421679	2421680	2421681	2421682	2421683

B Plots of NMR spectra

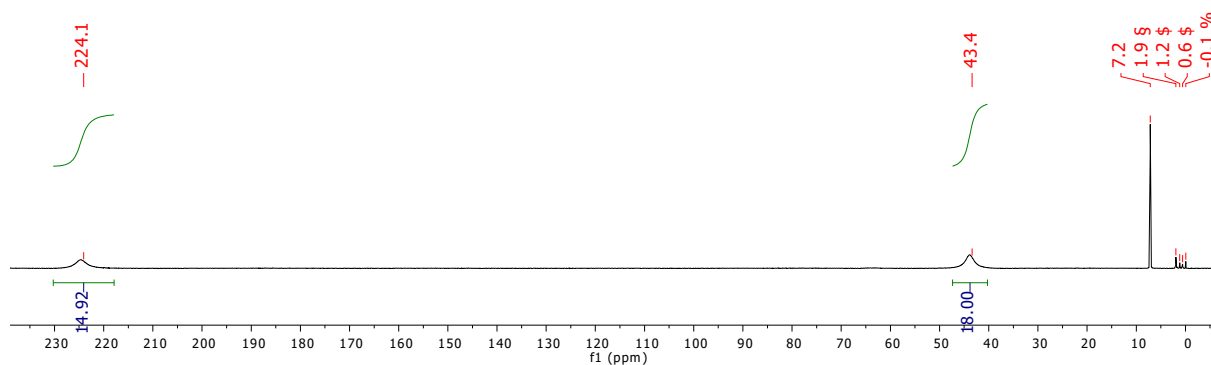


Fig. S1 ^1H NMR spectrum (400 MHz, C_6D_6) obtained with an analytically pure sample of $[\text{FeCp}^*\{\text{N}(\text{SiMe}_3)_2\}]$. Signals marked are due to small amounts of decamethylferrocene ($\text{\$}$), *n*-hexane ($\text{\$}$) and silicon grease (\%).

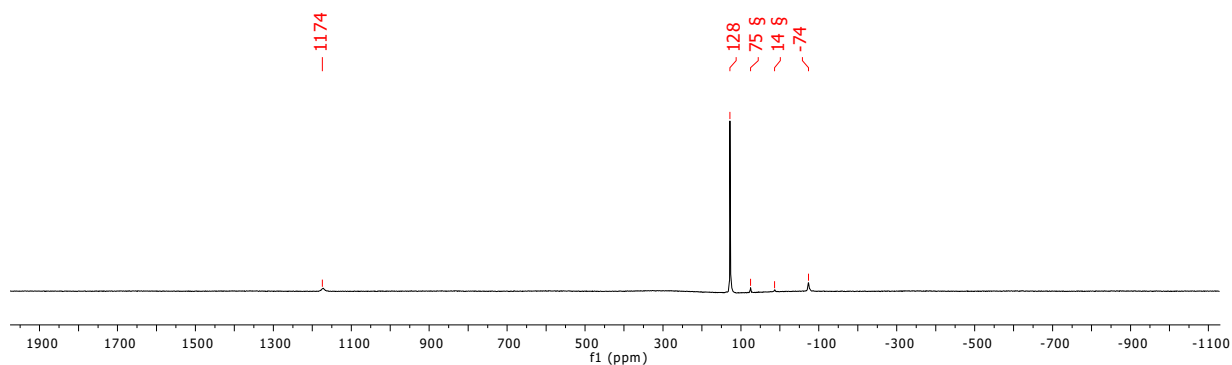


Fig. S2 $^{13}\text{C}\{^1\text{H}\}$ NMR spectrum (101 MHz, C_6D_6) obtained with an analytically pure sample of $[\text{FeCp}^*\{\text{N}(\text{SiMe}_3)_2\}]$. Signals marked are due to small amounts of decamethylferrocene ($\text{\$}$).

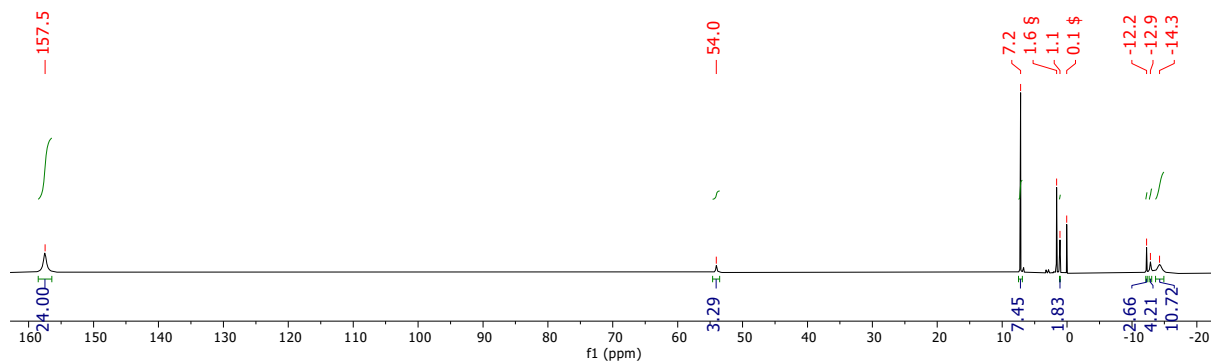


Fig. S3 ^1H NMR spectrum (500 MHz, C_6D_6) obtained with an analytically pure sample of **1**. Signals marked are due to small amounts of decamethylferrocene ($\text{\$}$) and silicon grease ($\text{\$}$).

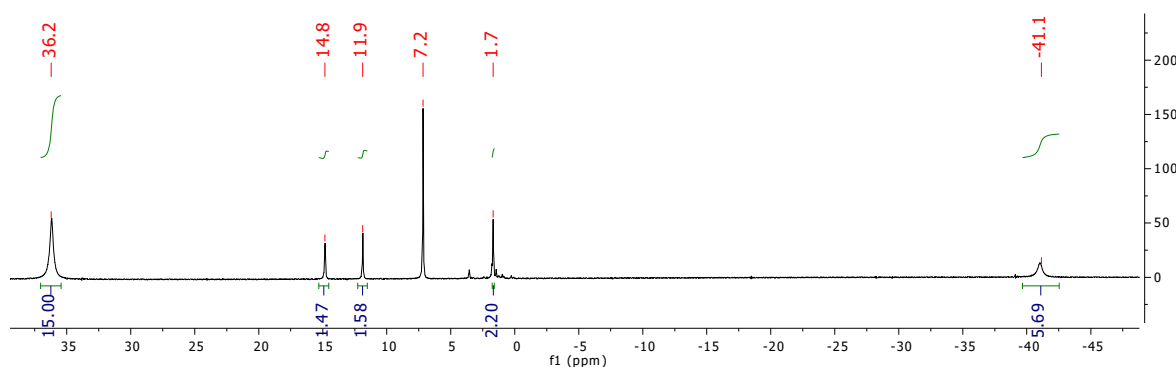


Fig. S4 ^1H NMR spectrum (400 MHz, C_6D_6) obtained with an analytically pure sample of **2**.

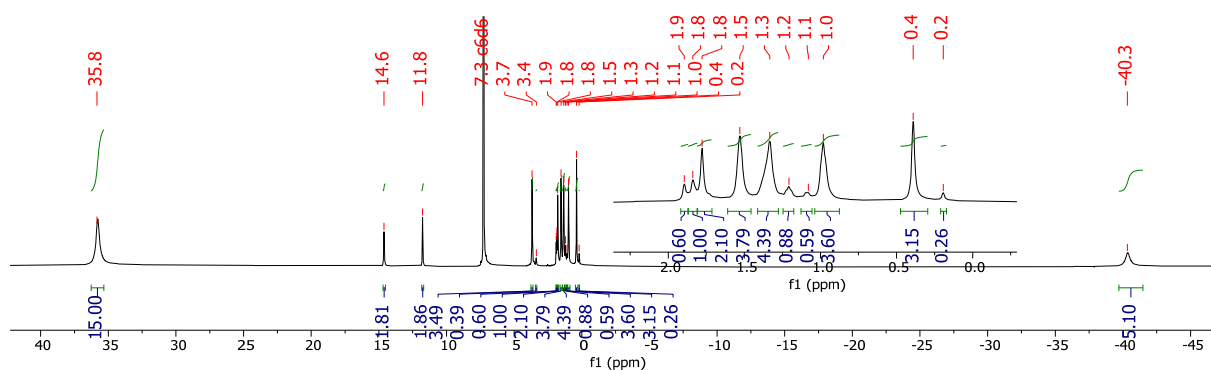


Fig. S5 ^1H NMR spectrum (400 MHz, C_6D_6) obtained with an analytically pure sample of **3**. The signals at $\delta = 36, 15, 12,$ and -40 ppm are assigned to **2** (formed from **3** in benzene solution).

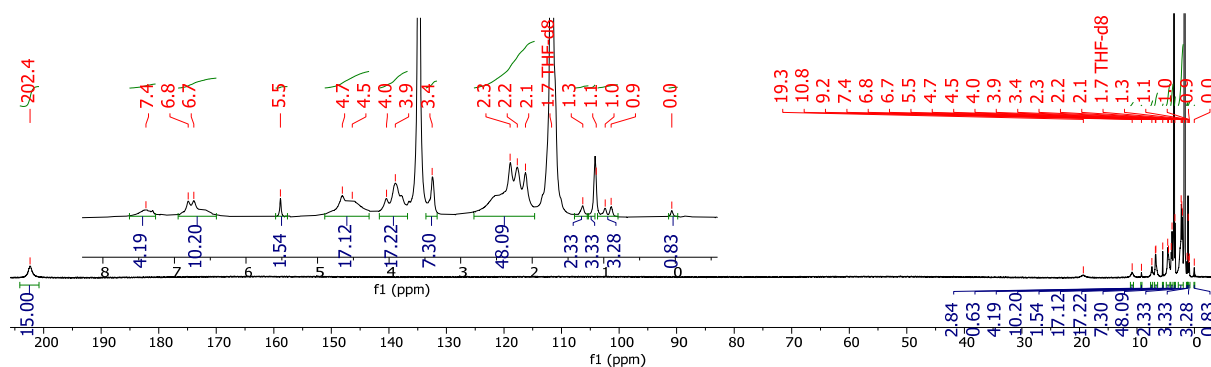


Fig. S6 ^1H NMR spectrum (500 MHz, THF-d_8) obtained with an analytically pure sample of **4**.

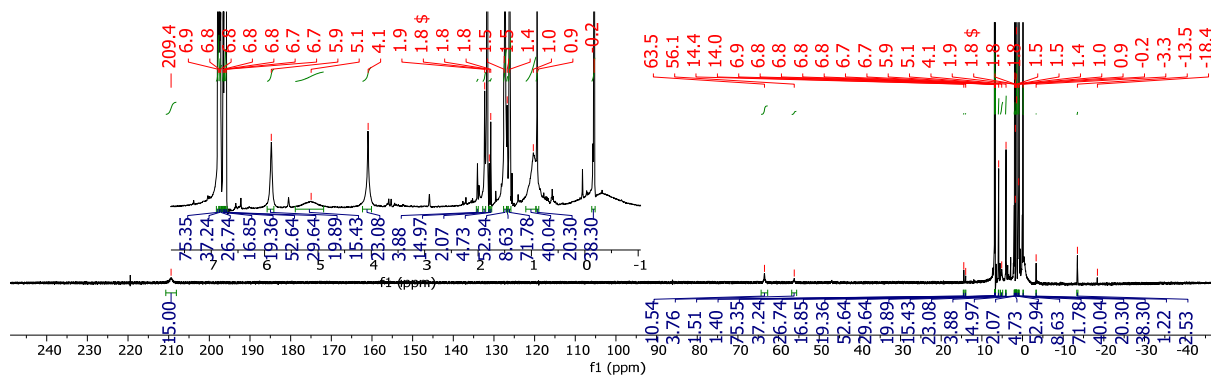


Figure S7. ^1H NMR spectrum (400 MHz, C_6D_6) of **5** (not analytically pure due to contamination with **4**). The signal marked belongs to decamethylferrocene ($\text{\$}$).

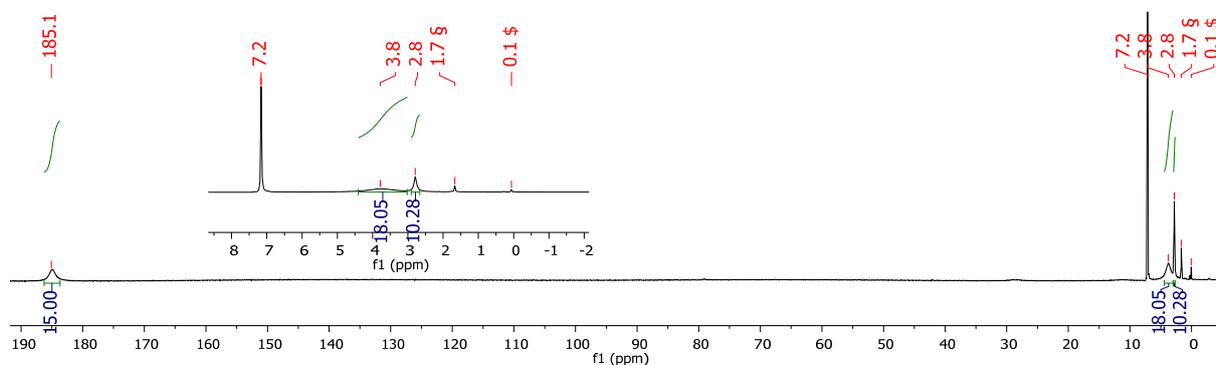


Fig. S8 ^1H NMR spectrum (400 MHz, C_6D_6) obtained with an analytically pure sample of **6**. The signals marked belong to decamethylferrocene ($\text{\$}$) and silicon grease ($\text{\$}$).

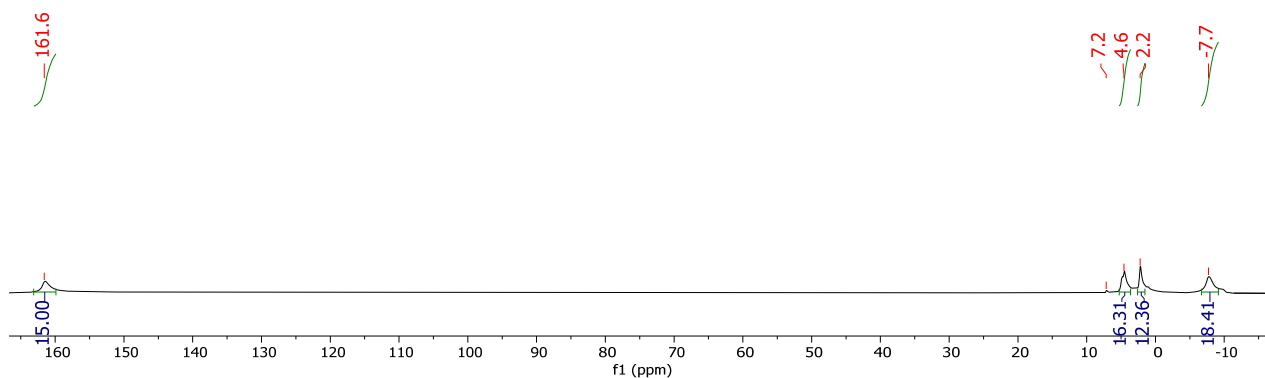


Fig. S9 ^1H NMR spectrum (500 MHz, C_6D_6) obtained with an analytically pure sample of **7**.

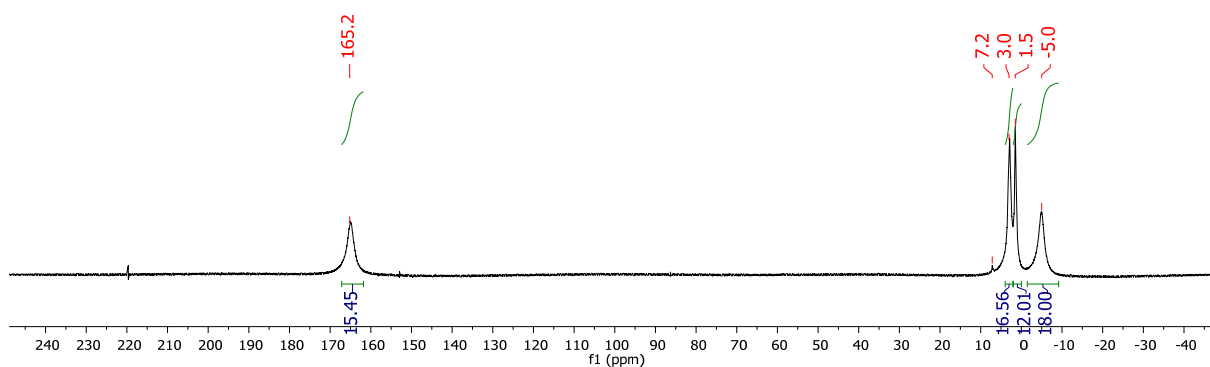


Fig. S10 ^1H NMR spectrum (400 MHz, C_6D_6) obtained with an analytically pure sample of **8**.

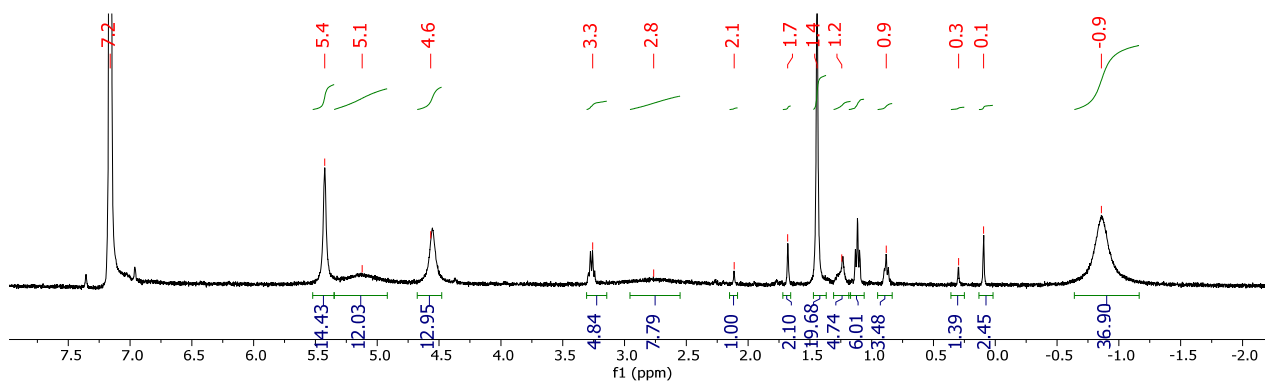


Fig. S11 ^1H NMR spectrum (400 MHz, C_6D_6) obtained with an analytically pure sample of **9**.

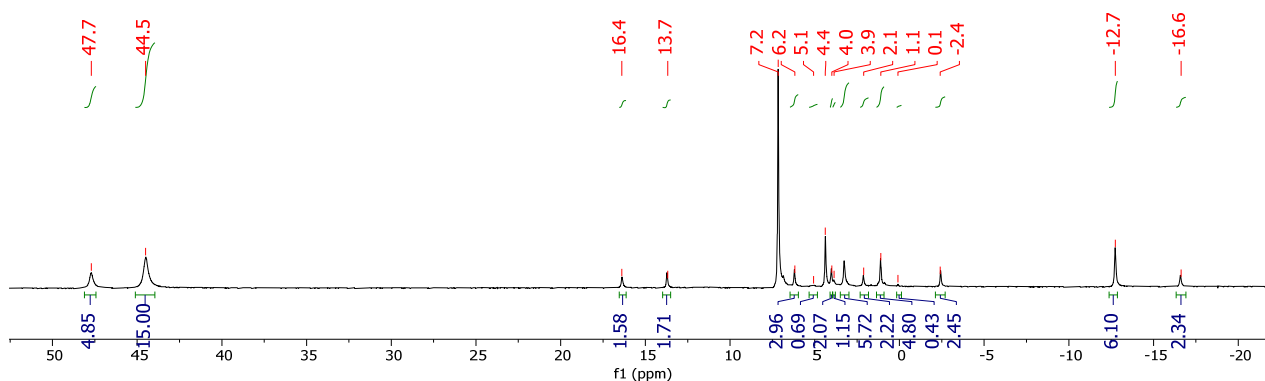


Fig. S12 ^1H NMR spectrum (400 MHz, C_6D_6) obtained with an analytically pure sample of **10**.

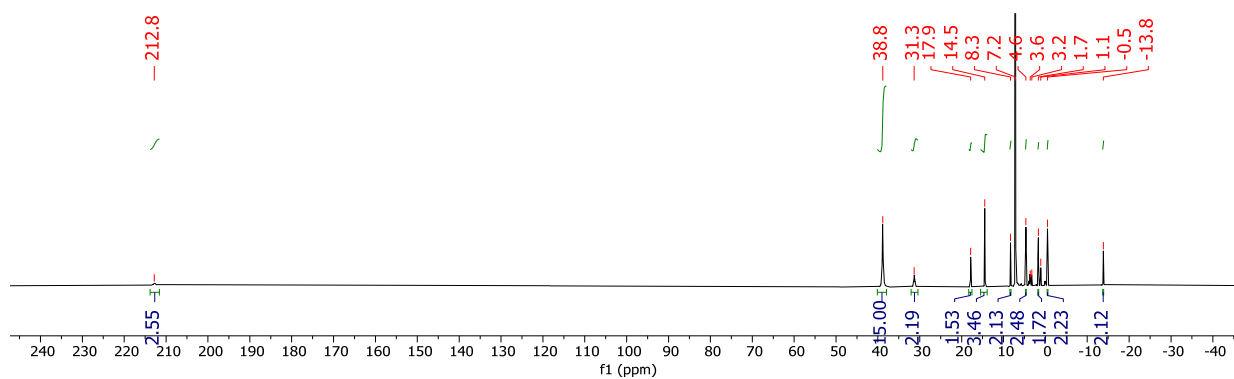


Fig. S13 ^1H NMR spectrum (500 MHz, C_6D_6) obtained with an analytically pure sample of **11**.

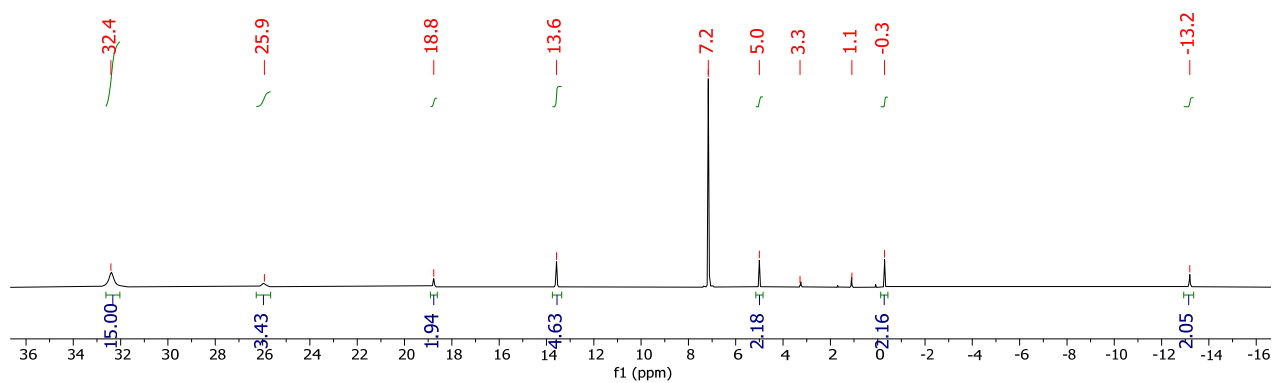


Fig. S14 ^1H NMR spectrum (500 MHz, C_6D_6) obtained with an analytically pure sample of **12**.

C Mößbauer spectroscopy

The Mößbauer spectrum was recorded with a ^{57}Co source in a Rh matrix using an alternating constant acceleration *Wissel* Mößbauer spectrometer operated in the transmission mode and equipped with a *Janis* closed-cycle helium cryostat. Isomer shift is given relative to iron metal at ambient temperature. Simulation of the experimental data was performed with the *MF* program using *Lorentzian* line sextets.⁵¹

D Magnetic measurements

Temperature-dependent magnetic susceptibility measurements were carried out with a *Quantum-Design* MPMS-XL-5 SQUID magnetometer equipped with a 5 Tesla magnet in the range from 2 to 210 K in a magnetic field of 0.5 T. The polycrystalline sample was contained in a gelatine capsule, covered with a few drops of low viscosity perfluoropolyether-based inert oil Fomblin Y45 to fix the crystals, and fixed in a non-magnetic sample holder. The maximum measuring temperature of 210 K was chosen because of the pour point of the oil, in order to keep the oil in the frozen state and to avoid therefore the orientation of the crystals parallel to the magnetic field. Each raw data file for the measured magnetic moment was corrected for the diamagnetic contribution of the capsule and of the inert oil according to $M^{\text{dia}} = \chi_{\text{g}}mH$, with experimentally obtained gram susceptibility of the capsule ($\chi_{\text{g}} = -5.70 \cdot 10^{-7}$ emu/(g·Oe)) and of the oil ($\chi_{\text{g}} = -3.82 \cdot 10^{-7}$ emu/(g·Oe)). The molar susceptibility data were corrected for the diamagnetic contribution according to $\chi_{\text{M}}^{\text{dia}}(\text{sample}) = -0.5 \cdot M \cdot 10^{-6}$ cm³ mol⁻¹. $\chi_{\text{M}}T$ vs. T data were modelled using a fitting procedure to the spin Hamiltonian for one iron(II) ion ($S = 2$) with Zeeman splitting and zero-field splitting (eq. 1).

$$\hat{H} = \mu_{\text{B}} \vec{B} \mathbf{g} \vec{S} + D \left[\hat{S}_z^2 - \frac{1}{3} S(S+1) \right] \quad (\text{eq. 1})$$

Full-matrix diagonalization of the spin Hamiltonian was performed with the *juIX_2s* program.⁵² Matrix diagonalization is done with the routine ZHEEV from the LAPACK numerical package. Parameter optimization is performed with the simplex routine AMOEBA from NUMERICAL RECIPES. A somewhat better fit was achieved when intermolecular interactions were taken into account ($zJ_{\text{inter}} = -32.9$ cm⁻¹, where z is the number of nearest neighbours). Temperature-independent paramagnetism ($TIP = 1750 \cdot 10^{-6}$ cm³ mol⁻¹) was included according to $\chi_{\text{calc}} = \chi + TIP$.

Frequency dependent ac magnetic susceptibility measurements of $[\text{FeCp}^*\{\text{N}(\text{SiMe}_3)_2\}]$ at various temperatures (Fig. S15) were performed to determine the relaxation barrier U_{eff} .

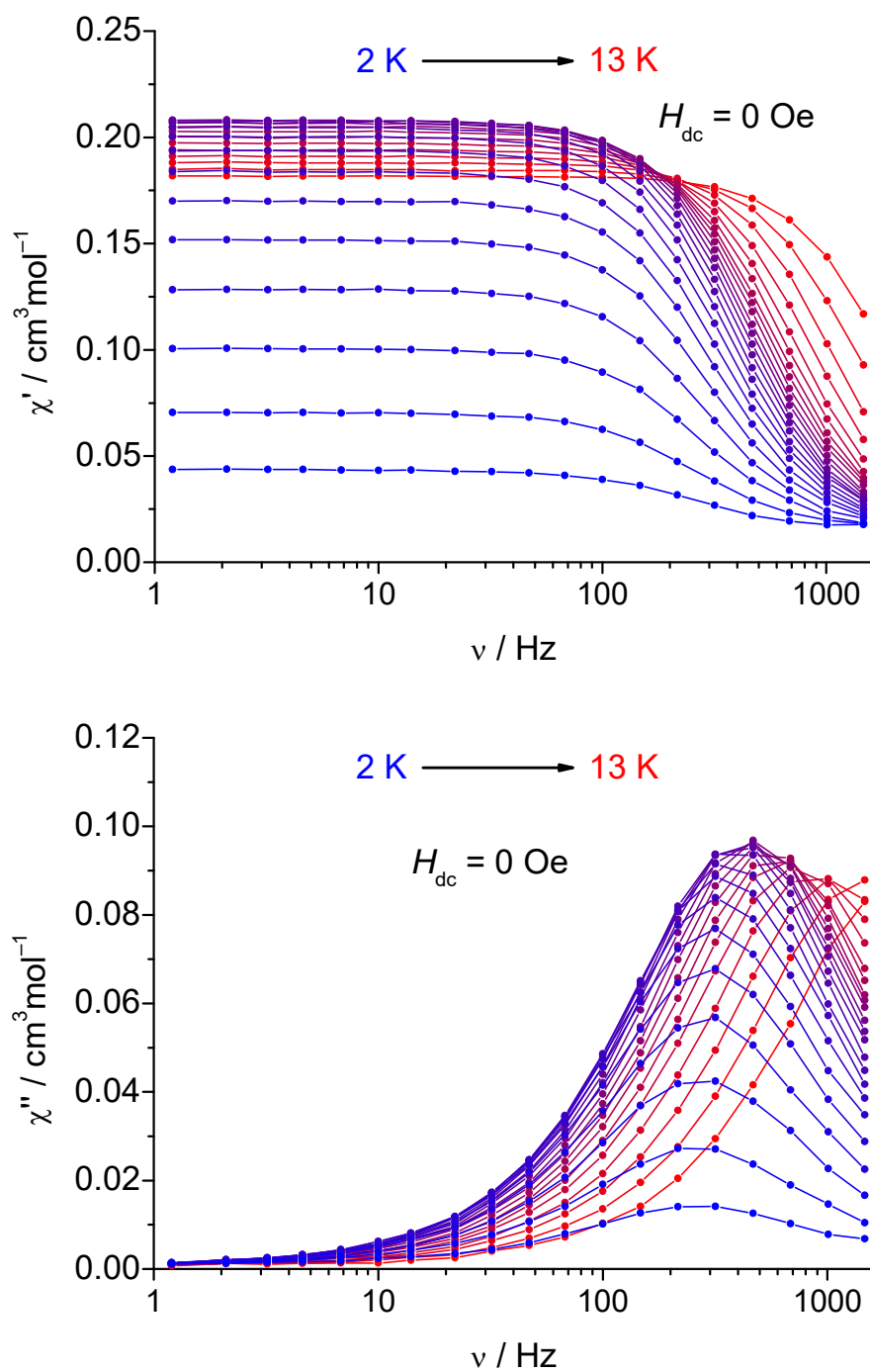


Fig. S15 Frequency dependence of χ' (top) and χ'' (bottom) at various temperatures in the absence of a dc field. The measurements were done between 2 and 13 K with steps of 0.5 K.

For this reason, the resulting χ' and χ'' values were used for constructing the Cole–Cole diagrams (Fig. S16) and simultaneously fitted using the CC-Fit program.^{S3}

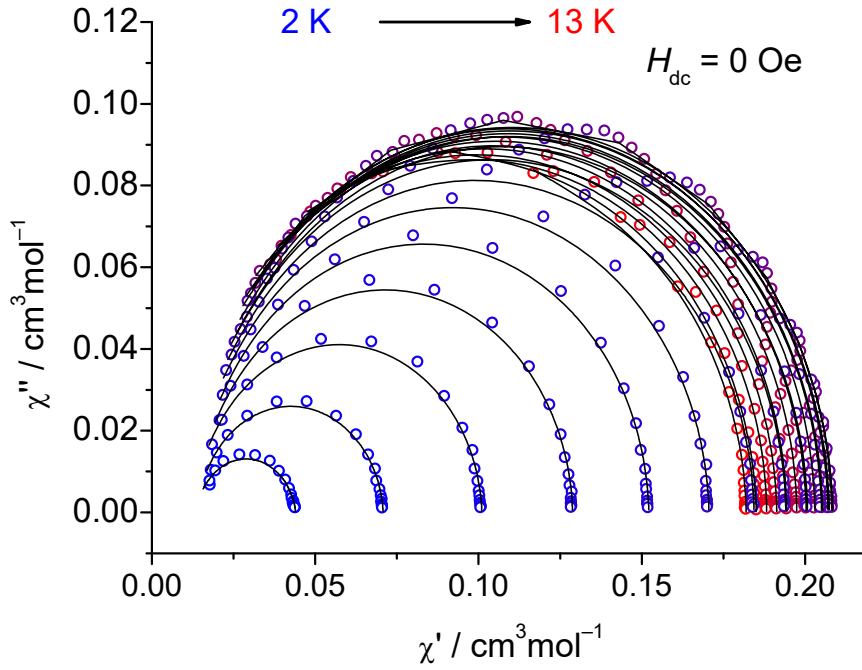


Fig. S16 Cole–Cole diagrams in the absence of a dc field between 2 and 13 K with steps of 0.5 K; the black solid lines represent the fit curves.

The temperature dependence of the obtained relaxation times τ is depicted in Fig. S17.

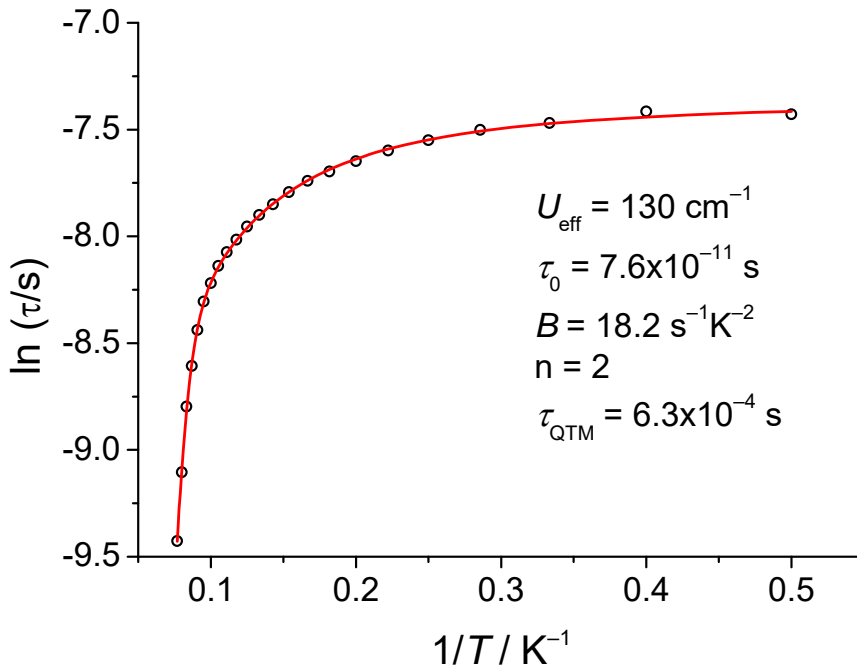


Fig. S17 Arrhenius plot of the temperature dependence of τ in the absence of a dc field.

The obtained points are clearly deviated from the linear Arrhenius law, so, additional relaxation processes have to be considered. In general, the temperature dependence of the relaxation times can be described according to (eq. 2) with three different types of relaxation: direct, Raman, Orbach processes and quantum tunneling of the magnetisation (QTM).^{S4} The direct term can be neglected since the relaxation is performed without external field.

$$\tau^{-1} = BT^n + \tau_0^{-1} \exp(-U_{\text{eff}}/k_B T) + \tau_{\text{QTM}}^{-1} \quad (\text{eq. 2})$$

The obtained best fit parameters are $B = 18.2 \text{ K}^{-2} \cdot \text{s}^{-1}$, $n = 2$, $U_{\text{eff}} = 130 \text{ cm}^{-1}$, $\tau_0 = 7.6 \cdot 10^{-11} \text{ s}$ and $\tau_{\text{QTM}} = 6.3 \cdot 10^{-4} \text{ s}$.

E References

- S1 E. Bill, *MF Program*, Max Planck Institute for Chemical Energy Conversion, Mülheim an der Ruhr, Germany.
- S2 E. Bill, *julX_2S, Program for Simulation of Molecular Magnetic Data*, Max Planck Institute for Chemical Energy Conversion, Mülheim an der Ruhr, Germany, 2014.
- S3 D. Reta and N. F. Chilton, *Phys. Chem. Chem. Phys.*, 2019, **21**, 23567–23575.
- S4 R. L. Carlin, *Magnetochemistry*, Springer-Verlag, Berlin, Heidelberg, 1986.